

Doi: 10.58414/SCIENTIFICTEMPER.2025.16.3.03

RESEARCH ARTICLE

Swarm intelligence-driven HC2NN model for optimized COVID-19 detection using lung imaging

Y. Mohammed Iqbal*, M. Mohamed Surputheen, S. Peerbasha

Abstract

COVID-19 virus has emerged as a formidable global health challenge, significantly complicated by the continuous evolution of viral variants that modify the virus's structural characteristics. Predicting disease affection in the lungs is complex and degrades the accuracy level of COVID-19 variants through imaging techniques, which remains a formidable challenge. The complexities involved in identifying these regions are exacerbated by issues such as image degradation, the high dimensionality of features, and scaling properties, all contributing to an increased rate of false positives. Consequently, this leads to decreased disease detection frequency, lower precision accuracy, and poor performance of traditional diagnostic methods, as reflected in reduced F1 scores and overall detection accuracy. To resolve this problem, enhanced Swarm intelligence-based optimal feature engineering with hyperscale capsule net-convolution neural network (HC2NN) was used to identify the survey of COVID-19 affection accurately. The preliminary process takes place to preprocess the covid-variant dataset with the support of adaptive Gaussian with wavelet filters. Then, iterative intra subset object scaling (I2SOS) is applied to identify the disease-affected region. Then, interrogative slice fragment clustering (ISFC) is used to segment the disease region. Throughout the disease region properties, the feature selection is applied with swarm intelligence, and identification is carried out by HC2NN work to effectively find the disease margin. The proposed experiment results project higher precision accuracy in prediction rate as well as in increasing true positives rate to attain the best recall, sensitivity performance, and F1 score. The novelty proves to have a higher performance than the existing traditional methods.

Keywords: COVID-19, Lung images, Feature selection, Dataset, Preprocess, Classification, Neural network, Machine learning, Clustering, Performance, Accuracy.

Introduction

Lung diseases impact a considerable number of people worldwide. People can develop a variety of severe lung conditions, such as TB, pneumonia, asthma, and fibrosis, to mention a few, Haennah, J. H. J., Christopher, S., & King,

Department of Computer Science, Jamal Mohamed College (Autonomous), Tiruchirappalli, Tamil Nadu, (Affiliated to Bharathidasan University), Tiruchirappalli, Tamil Nadu, India - 620 020.

*Corresponding Author: Y. Mohammed Iqbal, Department of Computer Science, Jamal Mohamed College (Autonomous), Tiruchirappalli, Tamil Nadu, (Affiliated to Bharathidasan University), Tiruchirappalli, Tamil Nadu, India - 620 020, E-Mail: mohammedit2k15@gmail.com

How to cite this article: Iqbal, T.M., Surputheen, M.M., Peerbasha, S. (2025). Swarm intelligence-driven HC2NN model for optimized COVID-19 detection using lung imaging. The Scientific Temper, **16**(3):3863-3874.

Doi: 10.58414/SCIENTIFICTEMPER.2025.16.3.03

Source of support: Nil **Conflict of interest:** None.

R. G. (2023). Coronavirus infections frequently start in the respiratory system, specifically the lungs. Early detection can improve the effectiveness of lung issues treatment.

Since there is currently no cure or vaccine for the rare COVID-19 disease, early discovery is crucial to minimizing infection risks to the general population and enabling the prompt isolation of the suspected person. Chest radiography, sometimes referred to as X-ray or computed tomography (CT) images, is a simple and quick way to diagnose COVID-19 and pneumonia.

During the early stages of COVID-19, a ground glass design is seen; be that as it may, it is difficult to spot this design near the pneumonic course borders. Topsy-turvy, sketchy, or broad aviation route opacities connected to COVID-19 have also been reported. It takes a team of highly trained radiologists to interpret changes in the body on such a small scale, (Mathesul, S., et al., 2023).

Medical imaging has drawn more attention to the computed-aided analysis of pulmonary diseases as deep-learning techniques have become more popular. Computed tomography (CT) scans can now be automatically analyzed to identify cancerous lesions. In turn, radiographic analysis

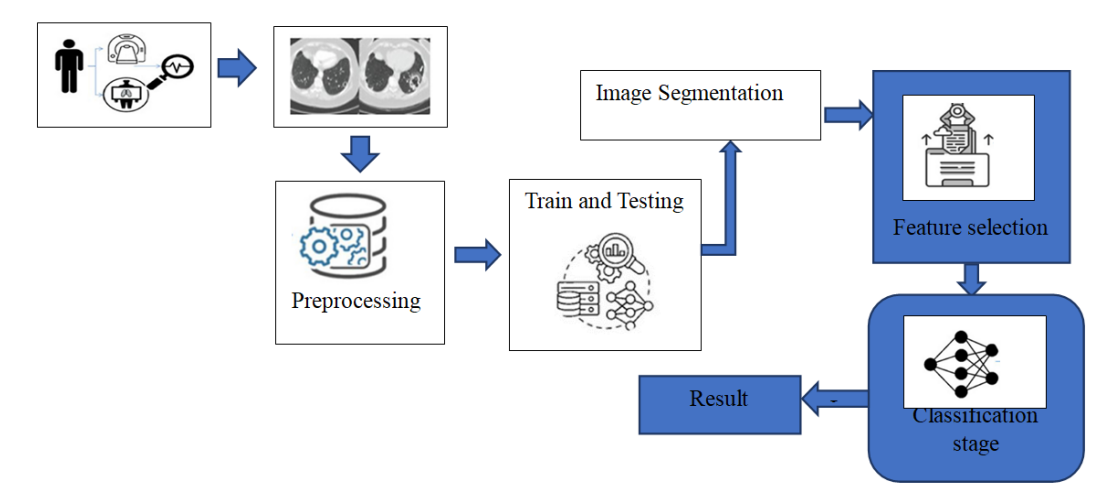


Figure 1: Introduction diagram

has shown good results in detecting various cardiothoracic anomalies and symptoms of tuberculosis.

A practical method for examining lung tissues, determining the stages of lung cancer, and categorizing these phases is visual image analysis. It is challenging to group it according to stages, though. However, lung cancer can be effectively classified using sophisticated deep-learning techniques. Figure 1 clearly illustrates the development of lung cancer and divides it into phases. Deep learning algorithms are used to distinguish and classify the various forms of lung cancer. The first stage in diagnosing and treating lung cancer is detecting the disease in the lung tissue, which is the most crucial and efficient procedure.

Lung cancer classification using deep learning techniques, with a particular emphasis on the most often used approach, the hyperscale capsulenet-convolution neural network (HC2NN). Its multi-layer construction, automatic weight learning, and ability to communicate local weights allow it to reach the highest precision. Deep learning models, algorithms, and techniques are crucial for improving accuracy and lowering errors in the categorization of lung cancer.

In many ways, automatic segmentation based on deep learning is superior to manual segmentation, Liu, S., & Yao, W. (2022). Deep learning produces high-quality images, lowers error rates, prevents misclassification, and correctly diagnoses cancer. Several classifiers are used to filter away false-positive nodules, Jiang, H., Ma, H., Qian, W., et al. (2017). The radiologist's ability to make a prompt and precise diagnosis is directly correlated with the quality and accuracy of the images. Additionally, deep learning techniques are used to forecast lung cancer. Features are automatically derived from training photos, Jiang, W., Zeng, G., Wang, S., et al. (2022).

Deep learning's HD representation of the input data helps the radiologist expedite the detection and identification process. Pixel bases are used to distinguish between cancerous and non-cancerous regions, so the pixels in the image help detect cancer right away. Therefore, by assisting physicians in the diagnosis and categorization of illnesses, deep learning benefits the healthcare system. It makes it easier to make accurate decisions about disease, Kumar, V., & Bakariya, B. (2021).

- Preprocessing removes noise and null values, and the Swarm intelligence and identification method is used to find the disease's associated features.
- The marginal rate data is used to select the best features of the disease based on the class labels.
- The hyperscale capsule net-convolution neural network method is used to classify the patient's lung disease affection.

Literature Review

Early identification is essential for respiratory infections to increase the effectiveness of therapies. To propose a lightweight network that uses lung noise to classify respiratory diseases, Banerjee, N., & Das, S. (2021). The LS signal's modes are examined using the empirical wavelet transform. The time-domain and frequency-domain characteristics of each mode have been obtained. Machine learning algorithms have been selected to automatically detect PDs based on the properties of LS signals, Roy, A., & Satija, U. (2023).

Physicians can use breathing sounds to diagnose a variety of respiratory system issues. Abnormal lung sounds, which have been clinically associated with disorders such as bronchitis and chronic obstructive pulmonary disease, are commonly associated with chronic respiratory diseases worldwide, Tripathy, R. K., Dash, S., Rath, A., Panda, G., & Pachori, R. B. (2022). Using respiratory sound recordings, diseases can be identified, and respiratory cycle abnormalities can be categorized. The system starts by

transforming input sound into a spectrogram representation using front-end feature extraction, Wu, C., Ye, N., & Jiang, J. (2024).

The utilization of deep learning strategies in clinical imaging on enormous datasets has permitted PC calculations to create as powerful outcomes as clinical experts. To help specialists, it is fundamental to have a flexible framework that can conveniently distinguish different illnesses in the lungs with high exactness. Over the long run, although numerous classifiers and calculations have been carried out, profound learning models (i.e., CNN, Profound CNN, and R-CNN) are known to offer improved results, Pham, L., Phan, H., Palaniappan, R., Mertins, A., & McLoughlin, I. (2021). Existing methodologies for examining respiratory sounds need space-trained professionals. This way, an exact and computerized lung sound grouping apparatus is required. In this paper, I have fostered a programmed demonstrative framework to characterize these signs. It can uphold medical care frameworks in low-asset conditions with restricted assets and a deficiency of qualified clinical experts, Irtaza, M., Ali, A., Gulzar, M., & Wali, A. (2024).

Computer-aided diagnostic (CAD) frameworks help radiologists make more accurate conclusions with less significant financial outlay by processing and presenting little data meaningfully. The goal of this research project is to propose a CNN and MHCNN-based framework for pneumonic illness identification based on CXR images that are better, more accurate, and more effective, Babu, N., Pruthviraja, D., & Mathew, J. (2024). One of the most deadly respiratory conditions is chronic obstructive pulmonary disease (COPD).

Muguli, A., Kumar, R., Nanda, V., Pinto, L. M., Ghosh, P. K., & Ganapathy, S. (2023).

It can be assessed using various clinical methods, including spirometric measurements, lung capacity tests, parametric reaction planning, wheezing episodes of lung sounds (LSs), and so on. Because LSs are associated with respiratory anomalies caused by aspiratory diseases, checking them is more effective for detecting respiratory problems, Zaidi, S. Z. Y., Akram, M. U., Jameel, A., & Alghamdi, N. S. (2021).

Early diagnosis is crucial for improving long-term survival rates and facilitating quicker recovery. Using deep learning techniques, lung disorders may be automatically, quickly, and accurately diagnosed from medical photos. Convolutional neural networks, particularly, have demonstrated promising results in diagnosing illnesses. However, the success of these supervised models depends heavily on the availability of a lot of labeled data, which can be expensive and timeconsuming to collect, especially for new diseases, Roy, A., Thakur, A., & Satija, U. (2023).

The accuracy of the current approaches on the two mentioned aspects is limited. This paper introduces algorithms for survival analysis and cancer subtype categorization using a multi-model deep learning framework. The platform includes two deep-learning pipelines for survival analysis and lung cancer type identification, respectively. An improved convolutional neural network (CNN) and multi-head CNN (MHCNN) model called LCSCNet is suggested to identify lung cancer subtypes automatically, Ozturk, T., Talo, M., Yildirim, E. A., Baloglu, U. B., Yildirim, O., & Acharya, U. R. (2020).

The accuracy of the current approaches on the two aforementioned aspects is limited. This paper introduces algorithms for survival analysis and cancer subtype

References	Proposed method	Drawbacks	Results
Yadav, P., Menon, N., Ravi, V., & Vishvanathan, S. (2023).	CXR deep neural Network (CXR- Net)	Unsuitable for diagnostic purposes.	Accuracy-0.95% Sensitivity-0.93%
Zhang, X., et al. (2023).	Refined Attention Pyramid Network (RAPNet)	manually identified	Pre-0.96% Rec-0.96.05% F1-0.98%
Vinta, S. R., Lakshmi, B., Safali, M. A., & Kumar, G. S. C. (2024).	CNN, R-CNN	Low accuracy	Recall-57% Accuracy-93.6%
Yu, H., Zhou, Z., & Wang, Q. (2020).	CNN-MoE	Cannot detect disease	Pre-0.98% Re-0.98.05% F1-0.94%
Ozdemir, O., Russell, R. L., & Berlin, A. A. (2020).	Residual Deep Neural Network (ResNet)	Not effective for identifying respiratory issues.	Accuracy-95.13% Sensitivity-96.33% Specificity-94.37%
Aharonu, M., & Ramasamy, L. (2024).	Adaptive Hierarchical Heuristic Mathematical Model (AHHMM)	earlier stage is challenging to predict	Accuracy-96.67%
Chetupalli, S. R., Krishnan, P., Sharma, N.,	CNN	High risk	Accuracy-97.67%

Table 1: Existing survey for lung disease detection using deep learning

categorization using a multi-model deep learning framework. The platform includes two deep-learning pipelines for survival analysis and lung cancer type identification, respectively. An improved convolutional neural network (CNN) and MHCNN model called LCSCNet is suggested to identify lung cancer subtypes automatically, Sanghvi, H. A., Patel, R. H., Agarwal, A., Gupta, S., Sawhney, V., & Pandya, A. S. (2023).

The model utilized a Long Short-Term Memory (LSTM) network classifier to encode time-frequency features and health symptoms, Bohmrah, M. K., & Kaur, H. (2021). Recent research has applied machine learning models like Naïve Bayes and SVM for predicting bipolar disorder cases. Studies highlight that deep learning methods enhance accuracy in mental health diagnosis, Peerbasha, S., Mohamed Surputheen, M. (2021).

However, collecting, evaluating, and analyzing vast quantities of health-related data—like images—is challenging and time-consuming for medical professionals. Lung cancer is among the many infectious and malignant diseases that artificial intelligence tools, such as machine and deep learning systems, help detect early, C. Wu, N. Ye and J. Jiang (2024).

A fine-tuned DensNet-201 model is proposed for the classification of chest X-ray images, Sanghvi, H. A., Patel, R. H., Agarwal, A., Gupta, S., Sawhney, V., & Pandya, A. S. (2023). The software uploads and analyzes chest X-ray images utilizing an enhanced detection model. Radiologists then receive disease classifications via DenseNet-201, allowing them to compare similar radiographs for verification, Bohmrah, M. K., & Kaur, H. (2021).

Problem Statement

When the size of the training set increases, existing algorithms render training algorithms inefficient. Many settings must be set precisely to get the best outcomes.

- It has a better solution for predicting Lung disease complications but has lower accuracy.
- It optimizes cancer prediction during the reduced test specificity and reduces the positive rates.
- Estimating effective cancer mortality risk from Lung disease-related genomic data is a major Challenge.
- Image identification accuracy values do not indicate feature relationships or classification mistakes.

Materials and Method

The most recent findings on deep learning-based lung image screening image for COVID-19 disease prediction will be presented. Image Processing consists of Covid lung disease segmentation, detection, classification, and image preprocessing. HC²NN classifier uses particular subset metrics to optimize feature selection. Its contribution is in combining subset features to increase classification accuracy. Categories are class labels, and feature selection is utilized in this section to identify data points depending on feature selection. It aims to increase the accuracy of lung disease predictive categorization. The level of error analysis and data time complexity are used to determine the prediction rate to improve prediction accuracy and recall.

Initially, I collected the images from the standard repository and started the preprocessing stage to reduce the Noise ratio and unbalancing values; the second step is segmenting the images to identify the affected Region based on interrogative slice fragment clustering (ISFC) and iterative intra subset object scaling (I²SOS). The feature remains to convey features with marginal weight based on swarm intelligence. The HC2NN classifier categorizes lung disease features in Figure 2.

Image Dataset Collection

This data collection on common lung disorders, COVID-19, and other lung conditions is released in phases, as illustrated

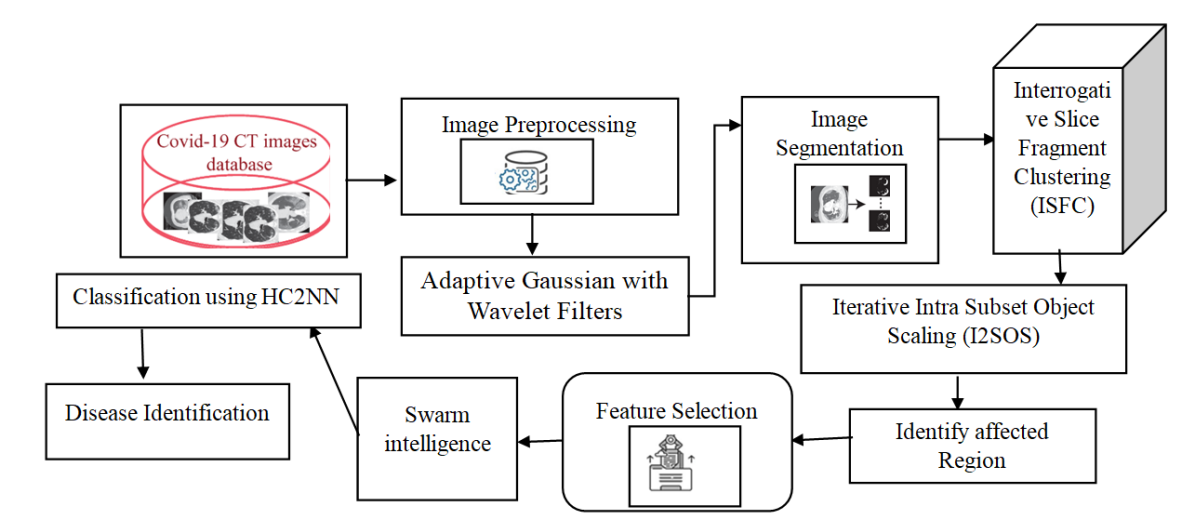


Figure 2: Proposed diagram

in Figure 3. 217 Covid-19, 1,340 conventional, and 1,344 viral pneumonia chest X-ray (CXR) images are included in the initial distribution. In this initial release, 1,201 CXR images were added to the COVID-19 category. This second database update includes 1,345 lung masks associated with viral pneumonia images, 6,012 non-COVID-19 lung opacities, 10,192 standard cases, and 3,616 COVID-19 positive cases. As additional Covid-19 pneumonia patient scans become available, this database will be updated.

Image Preprocessing

Preprocessing lung CT scans enhances their quality and improves lung nodule diagnosis outcomes. Improving the image is crucial since the lung has numerous features that could be mistaken for tumors. Datasets on Lungs were gathered using imaging screening records and at varying fitness levels. Adaptive Gaussian with wavelet filters uses the identified list of features to confirm that all of the elements in the list of features have attributes and values. A lung disease identification and analysis process will eliminate missing or partial drops.

The Gaussian filter minimizes group latency in this manner. In terms of mathematics, a Gaussian filter connects and applies a Gaussian function to the input signal. Gaussian filters are the prevalent smoothing technique. The next logical step is wavelet analysis, a windowing method that uses zones of different sizes, as shown in Figure 4. When more accurate low frequencies are needed, frequency analysis enables you to use longer time intervals.

The Gaussian filter (multi-view medical imaging) is created using the input images. Using a 5 x 5 2D separable Gaussian filter $\omega(m\times n)\omega(m\times n)$, the source images are convolved to produce PlPl from bottom to top via downsampling. I stands for the current layer, G_z for the Gaussian, and W for the current number of rows in the I-th layer.

$$G_{z}(m*n) = 4 \sum_{m=-2n=-2}^{n} \sum_{n=-2}^{n} \omega(m*n) G_{l-1}(2_{i} + m, 2_{j} + n)$$

- 1: Input Lung screeningimage
- 2: Read images (Im) \rightarrow P(m,n)
- 3: Gaus-Wvlet filter forpixel to smoothing the Img (I) For both (Im)→Img 1..n

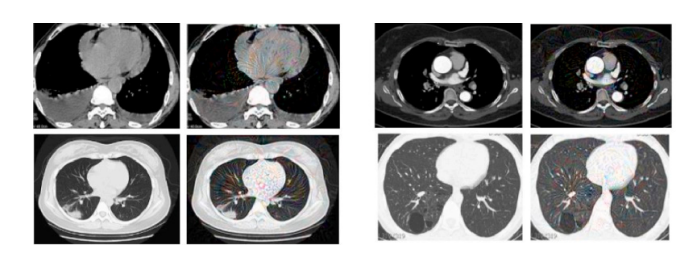


Figure 3: Dataset collection

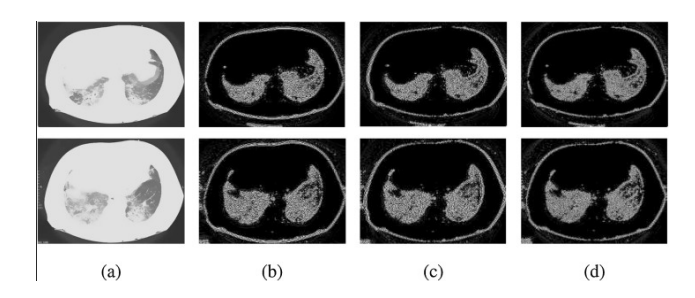


Figure 4: Gaussian Wavelet filter process

$$I(m,n) = e^{\frac{s^2(m,n)}{2\sigma^2}}$$
 , have the pixel value

To estimate the image values $\frac{1}{\sqrt{2\pi\sigma}}e^{\frac{-s^2(m,n)}{2\sigma^2}}$ 4: Return the images $Pc \leftarrow P(m,n)$

5: Reduced noise

End

An image preprocessing distance R(m,n) from the approach places the image change component of the matrix image, while the response and Gaussian filter analysis are centered on the σ runs. Using the first stage of the preparation procedure, the processes remove null reduction from the dataset and reduce image noise.

Segmentation using Interrogative Slice Fragment Clustering (ISFC)

A slice fragment is used to process the image on which noise sources have had an impact. First, the non-causal Region will be used to calculate the pixel and non-causal linear prediction error. Segmenting pixels using cluster in slicing fragment. In order for pixels to cluster with their neighbors, it is crucial to take into account the spatial relationships between them. For every pixel, pixel proximity is chosen in the same manner. The data's visible structure. A pixel's proximity is determined by considering how similar its spectrum is to that of nearby pixels.

Segment region (Sr)
$$S_{(5 \times 5)} = Img(x, y)$$
, $i-2 \le x \le i+2$, $j-2 \le y \le j+2$

Region of pixel maxi.point = inside the processing region of images.

$$I(x, y) = [Img(u, v)R, I(x, y)B]$$

Were x, y, and the lung screening image should have non-gradient pixels in every pixel. Pixels and their environment are closely related. The technique determines the present pixel value by combining the neighboring noisy and clear pixels in a weighted linear manner.

Figure 5 defines clustering segmentation as recognizing irregular areas in lung images and categorizing cancer according to their features.

Each lung objects mentioned f(x, y),

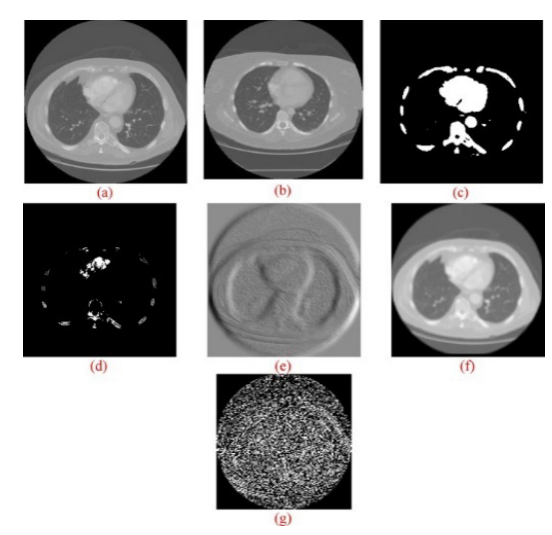


Figure 5: Segmentation using clustering

$$m_{pq} = \sum_{-\infty}^{\infty} \sum_{-\infty}^{\infty} x^{p} y^{q} f(x,y) dx dy$$
 p, q=0, 1, 2.

$$u_{pq} = \sum_{-\infty}^{\infty} \sum_{-\infty}^{\infty} (x - \overline{x})^p (\overline{y})^p s - if(x, y) dx$$
 p, q=0, 1, 2

Where \overline{x} and \overline{y} - images fusion metrics defined the achieved segment point

$$\overline{x} = \frac{m_{10}}{m_{00}}; \text{ and } \overline{y} = \frac{m_{01}}{m_{00}};$$

Used to create normalized central point corrective segments at the Region s(x, y) provide o's and 1's for variant and invariant segment points.

The segmentation algorithm combines background and temporal subtraction to segment moving objects and uses image space. Find the current pixel where R (x, y) belongs to the fragment images.

$$P_{xy} = \frac{R_{xy}}{R_x R_y}$$

$$R_{xy} = \frac{\sum xy}{n}$$

$$R_x = \sqrt{\sum x^2/N}, R_x = \sqrt{\sum y^2/N}$$

Where, P_x yx (where, a=x, b=y) X={a}, Y={b}, Each node calculated for each pixel of the borders. $\frac{R_x}{R_xR_y}$ -is the standard deviation of image values in a pixel.

Iterative Intra Subset Object Scaling (I²SOS)

Iterative Intrasubset Object Scaling (I2SOS) is a simple, fast-

integrating, and extremely dependable technique. This method's primary benefit is its simultaneous extraction of texture feature categorization and lung screening image information.

Compute the properties of a scaling-image-based system for recognizing lung clusters. Lung images are transformed into lung screening image textures. In the photographs balancing the separate lung screening image elements, each image identifies the characteristics and optimizes the image feature weights.

Each image is represented using the in-depth learning approach, which regulates each aspect to the weight of training models described by the current weak textured image once the weight has been correctly categorized for using the scaling objects.

To determine the object scaling of the covered pixel scaling region p(s), the highly scattered image approaches the point where it gains the probability index

The image's brightness with a greater mean rate When the lung image feature is chosen, the general brightness is obtained by using the low dissimilar 'L' in the grey range from 0 to 1 at the standard point to calculate the mean weight.

$$\dot{s} = \sum_{s=0}^{L-1} P(s) = \sum_{s} \sum_{s} \frac{I(r,c)}{M}$$

The low-brightness pixels were separated from the rows and columns of the pixel image, which had a constant equation variance. As a result, the object scaling levels, which are represented as a square root variation of the total number of pixels, were improved.

$$\sigma_{s} = \sqrt{\sum_{s=0}^{L-1} (S - \overline{S})^{2} L(g)} = \frac{1}{\sigma_{s}^{3}} \sum_{s=0}^{L-1} (S - \overline{S})^{3} L(S)$$

For every object value, linked pixels provide the coordinated mean and the inverse average point of the expected standard deviation rate.

Swarm Intelligence Using Feature Selection

In Swarm Intelligence feature selection, particles are represented as n-bit strings, where n is the dataset's total number of features. The d^{th} feature will be chosen, indicated by the position value of the dth dimension, or xid, which is [0,1]. To determine whether to choose features, a threshold x is applied. Choose the dth feature if xid > 0. The dth feature won't be selected differently.

Static weights in the range [0.8, 1.2] use constant values to optimize the algorithm. To improve PSO's optimization ability, it is recommended that the static weights be making selected. (1)

At the beginning of the PSO process, a high global search

efficiency enables new domains to be discovered.

$$w(x) = \frac{Iteration_{max} - x}{Iteration_{max} max} (w_{max} - w_{min}) + w_{min}$$

$$w(x) = \frac{Iteration_{max} max}{Iteration_{max}} (w_{max} - w_{min}) + w_{min} * A$$

 $Iteration_{max}$ Is the maximum number of iterations, and t is the current iterations of the algorithm.

The balance between global and local exploration determines the outcome of an optimization algorithm. The inertia weight w is a vital parameter set to an appropriate value to balance global and local utility. High values of w encourage global exploration; low values promote local development in Bi (t+1),

The provided feature selection technique considers features as a graph model, calculates centralities for all nodes, and uses a swarm-based search process to select the final set of features.

$$w(x) = w_{max} - (w_{max} + w_{min})$$

(ax) is decreased linearly from w_m ax at the early iterations to w in at the later. The behavior of these features.

$$w(x) = \left\{ w_t = \frac{w_{min} + w_{max}}{2} + \frac{w_{min} - w_{max}}{2} \cos\left(\frac{2\pi x (4a + 6)}{T}\right) \right\}$$
$$w(x) = w_{max} + (w_{max} - w_{in}) X \log_{10}\left(a + \frac{10x}{T}\right)$$

A single parameter in swarm intelligence controls this balanced weight (w). Even with fewer than half of the functionalities, the network can function effectively. Memory is a hidden state. The network advances it based on the inputs that are provided. The input and the previously hidden state value are the two variables used to calculate the new hidden state if you follow the arrow toward the hidden state value. U, V, and W denote different layer parameters. Although these parameters differ between layers, each layer utilizes the same values.

$$S_x = \sigma \left(w_{xy} x_a + w_{xy} y_a + B_x \right)$$
$$y_x = w_{xy} x_a + B_y$$

The σ function in the formula above represents nonlinearity, b is a bias form, and w is a weight matrix. Weight matrices come in a variety of forms, and each one has a unique explanation. The input value an is mapped to the hidden state value x via wxs. Along the time axis, the wss converts the value of the hidden state s to another hidden state value. For example, wsy transfers the hidden state value to an output value y between x1 and x2. Additionally, there are constant biases, which are represented by the symbols bs for the concealed state and by for the output, respectively. This bias vector can vertically shift any value going through the activation function.

Classification using Hyper scale Capsulenet-Convolution Neural Network (HC2NN)

The lung images are scaled variably according to hyper-scale dependencies, which results in variations in the feature threshold limits and dense features. To determine the closer weights on each hidden dense layer, the neural network is processed repeatedly, and the margins are iterated. Hierarchical connection modeling can be improved with this method. CNN drastically reduces the network's parameters by using repeated weights and biases across the whole layer. CNN applications through the use of specific topologies, like local connections and shared weights.

Pooling reduces the feature maps' resolution, ensuring invariance. Neurones merge a little $N \times N$ (for example, N = 2) segment of the convolution layer in the pooling layer. The most used pooling technique is max pooling.

Employed to train every parameter of the deep CNN model. CNN extracts features, which are subsequently sent into the deep capsule network for further processing.

Capsule Network (CN)

The capsule network modifies the conventional neural network, which employs a collection of neurons to learn the vector representations of a certain kind of item.

The weighted sum of the prediction vector uj|i from the preceding layers is the input to a capsule sj. The previous capsule's uj is multiplied by a transform matrix to create uj|i. Wij

$$sj = \sum_{n} u_{j|i} cij$$

Where *cij* stands for the coupling coefficients that are established by a method known as dynamic routing, after determining the entity's probability based on the output vector's length, the capsule applies a nonlinear function known as the squash function to squash the vector.

In addition to providing the entity's orientation, the vector representation employs the activity vector's length to determine the entity's probability. The pooling layer, which is used in conventional CNNs to maintain the network insensitive to tiny input changes, is restricted.

CNNs typically perform worse in classification because they are less resistant to translation, rotation, and scale. The output of a capsule network is a vector representation of a certain kind of entity. The length of the capsule's associated output vector might not alter much when the entity is changed. Utilizing the capsule network can get a more reliable representation of the input.

CNN is built using dense points and an integrated activation function for logical decisions.

$$i_t = s(w_x x_t + w_h h_{t-1} + w_c c_{t-1} + b_i)$$
 and

$$f_{t} = s \left(w_{fx} x_{t} + w_{hf} h_{t-1} + w_{cf} c_{t-1} + b_{f} \right)$$

$$h_t^{(1)} = x_t w_{xh}^{(1)} + h_{t-1} w_{hh}^{(1)} + b_h^{(1)}$$

$$h_{t}^{(2)} = x_{t} w_{h}^{(2)} + h_{t-1} w_{hh}^{(2)} + b_{h}^{(2)}$$

The hidden layer activation is as follows.

$$h_{t} = \left(mod\left(h_{t}^{(1)}\right) + mod\left(h_{t}^{(2)}\right)\right) / 2$$

The output is given by

$$y_t = w_{hv}h_t + b_v$$

 W_{hh} as identity as in HC2NN, $w_{hh}^{(1)} and w_{hh}^{(2)} b_h^{(1)} and b_h^{(2)}$ set as zero. Using threshold margins, this optimized recurrent neural network determines if a lung ailment is a high risk or low risk.

Result and Discussions

The results of the proposed feature selection using HC2NN will be compared with the training features of the lung imaging dataset. At this point, memory and precision are assessed through performance reviews. The final error rate's true/false condition is used to compute text case metrics. To analyze the competence of developed COVIDNet-Predictor, a comparative evaluation is carried out with baseline models such as CNN, MHCNN, and LSTM, DenseNet and Darknet. The performance measures including accuracy, specificity, recall, precision, and F1-score are employed to estimate the efficacy of proposed COVIDNet-Predictor

A lung imaging dataset is analyzed to evaluate the efficacy of the suggested approach. The number of test and train photos is used to evaluate texture detection for classification in lung images.

Python implements the suggested COVID-19 detection method with the enhanced HC2NN model on an Intel Core i3 processor 7,020U@2.3GHz, with 8GB of RAM and a 64-bit operating system. Activation is done using lung CT scans. The suggested method classifies COVID-19 images by comparing the training and test profiles of the proposed ResNet 101 70:30 for testing purposes. Simulation findings demonstrate the effectiveness of the suggested COVID-19 detection approach. Existing models such as CNN, RobNET, and RESTNET are used here.

This class is primarily responsible for the sharp increase and decrease because there were fewer COVID-19 instances than in the other two classes (Yes and No). By analyzing every CT scan for every training epoch, these high and low points in the training can be reduced.

• True negative (TN): An appropriately diagnosed normal lung image.

- True positive (TP): The case has been appropriately identified.
- False negative (FN): A mistaken identification of the case.
- False positive (FP): An inaccurate diagnosis is made based on normal lung imaging.

Evaluation Metrics

This class is primarily responsible for the sharp increase and decline because it had fewer COVID-19 cases than the other two (Yes and No). By evaluating every CT scan for each training cycle, these high and low moments in training can be decreased.

Accuracy measures how well the model performs overall across all classes. The proportion of accurately predicted samples to all samples in the dataset determines how it is computed.

$$\begin{array}{l} \textbf{computed.} \\ \textbf{Accuracy} = \frac{True_{pos} + True_{neg}}{True_{pos} + True_{neg} + False_{pos} + False_{neg}} \end{array}$$

$$Precision = \frac{True_{pos}}{True_{pos} + False_{pos}}$$

$$Recall = \frac{True_{pos}}{True_{pos} + False_{neg}}$$

$$F-measure = \frac{2*Precision*Recall}{Precision+Recall}$$

Figure 6 depicts the detection model's performance via a confusion matrix. Contains information about the model's strengths and flaws, including the number of True Positives (TP), False Positives (FP), True Negatives (TN), And False Negative (FN) predictions.

Experimental Results

For our investigation, we combined three publicly accessible chest X-ray datasets. Four labels were applied to the merged dataset: COVID-19, non-COVID-19, bacterial, and normal. We classified the labels as either positive or negative because our study's primary goal is to identify positive COVID-19 cases.

Using all of the data, a COVID-19 identification model based on HC2NN is then created. The collection's chest X-ray images were all shrunk to a uniform 100x100 pixel size. The input layer, which represented 128 × 128 x 3 RGB images, is the first layer of the HC2NN model. Using pre-trained models, transfer learning is applied to the COVID-19 dataset.

The tensor is converted to a vector using the compressed layer, and this vector is subsequently supplied to a fully interconnected neural network classifier.

A dropout of 0.5 is utilized to keep away from overfitting. The model is additionally enhanced by the result layer utilizing the Adam Optimiser. Irregular inspecting is used to isolate the first dataset into preparing and testing datasets. To work on the information during preparation, the preparation images were arbitrarily interpreted, flipped, and

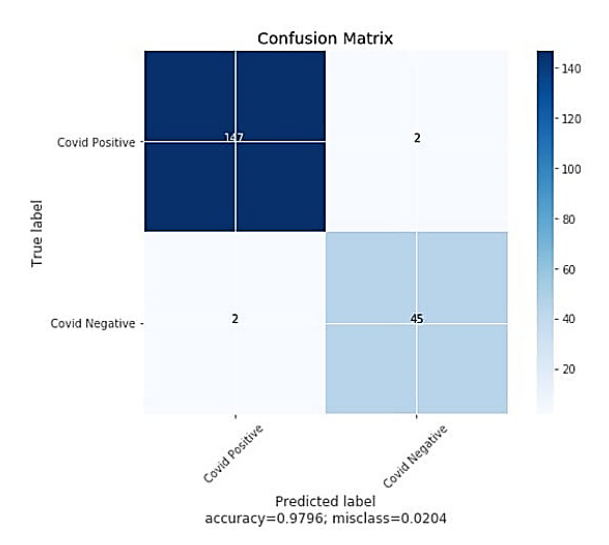


Figure 6: Confusion Matrix

pivoted. These qualities were experimentally obtained after each model was prepared for 50 ages with a group size of 32. Furthermore, the Adam streamlining agent's learning rate is experimentally discovered. A confusion matrix developed by analyzing more than 2900 correct X-ray scans is used to assess the COVID-19 detection model's performance.

Table 2 shows the performance of COVIDNet-Predictor over other baselines and models. The accuracy of the developed COVIDNet-Predictor and HC2NN techniques is high, at 95.04% and 97.9%, respectively, compared with existing models, which are 97.74%, 97.02%, 98.02%, 98.02%, and 96% better than CNN, DenseNet, Darknet, MHCNN, and LSTM, respectively. As for recall, precision, and F1-score, the proposed model attained better performance and outperformed other models.

Figure 7 shows the actual positive accuracy precision values when contrasting the various methods. Compared to other algorithms, the suggested implementation performs better. The proposed method, HC2NN, has a higher precision of 98.02% than the standard approaches, which have a CNN of 91.21%, a DenseNet of 93.6%, a DarkNet of 90.15%, a MHCNN of a 91.25%, LSTM of 90.01%, and a COVIDNet predictor of 97.85%.

Figure 8 shows recall performance data for True Positive Recall Accuracy. The recommended implementation

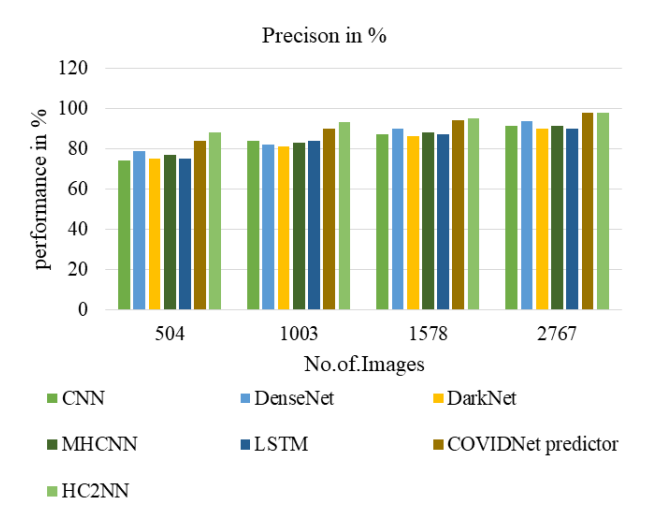


Figure 7: Precision performance

performs better than other algorithms when comparing the various methods. CNN of 92.4%, a DenseNet of 90.98%, a DarkNet of 95.14%, a MHCNN of a 95.15%, LSTM of 93.22%, and a COVIDNet predictor of 97.78%in the current approaches, while HC2NN, the suggested method, has an accuracy of 97.94%, which is higher than previous methods.

Figure 9 shows detection accuracy performance for comparing various approaches; the suggested implementation performs superior to other methods. The existing approaches have a CNN of 93.45%, a DenseNet of 94.14%, a DarkNet of 92.51%, a MHCNN of a 91.62%, LSTM of 92.41%, and a COVIDNet predictor of 95.0%. However, the proposed method, HC2NN, has a higher 97.9% accuracy than earlier methods.

Figure 10 shows detection specificity performance for comparing various approaches; the suggested implementation performs superior to other methods. The recommended implementation performs better than other algorithms when comparing the various methods. The CNN of 93.21%, a DenseNet of 94.68%, a DarkNet of 93.11%, a MHCNN of a 90.32%, LSTM of 91.01%, and a COVIDNet predictor of 96.91% in the current approaches, while HC2NN, the suggested method, has an accuracy of 97.02%, which is higher than previous methods

Figure 11 displays false rate statistics when comparing various methods; the suggested solution performs better

Table 2: Performance of COVIDNet-Predictor and HC2NN over Other Baseline and Models

Methods	Accuracy	Recall	Specificity	Precision	F1-score
CNN	93.45	92.4	93.21	91.21	92.14
DenseNet	94.14	90.98	94.68	93.6	93.84
Darknet	92.51	95.14	93.11	90.15	92.21
MHCNN	91.62	95.15	90.32	91.25	91.34
LSTM	92.41	93.22	91.01	90.01	90.18
COVIDNet-Predictor	95.04	97.78	96.91	97.85	95.88
HC2NN	97.9	97.74	97.02	98.02	96

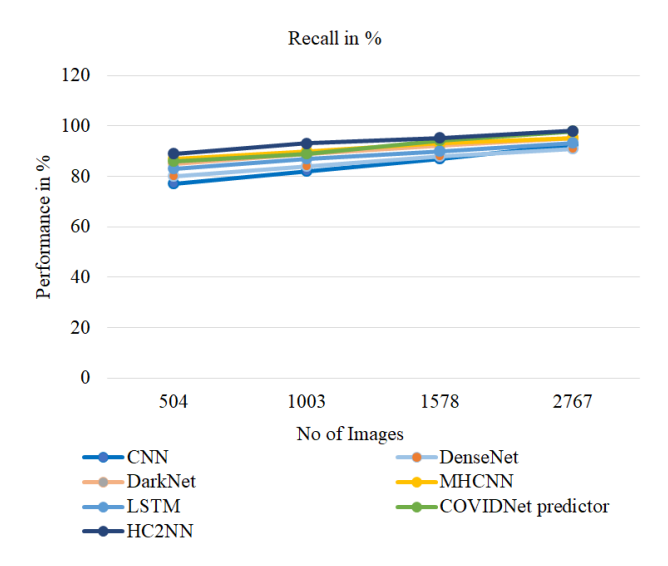


Figure 8: Recall performance

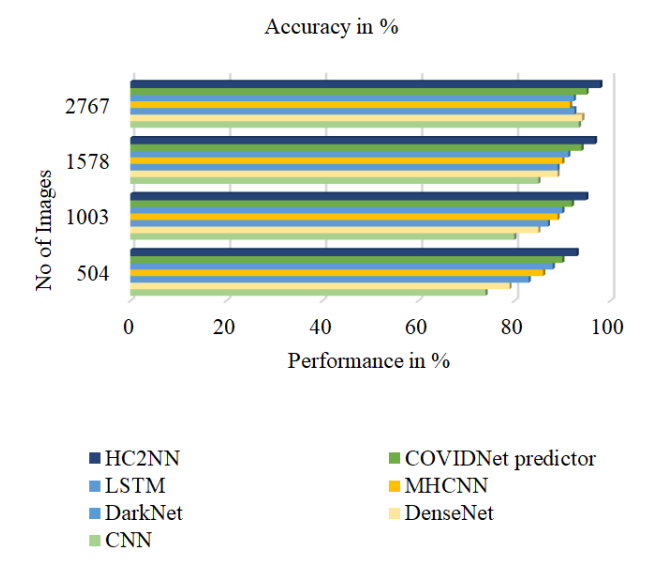


Figure 9: Analysis of Detection accuracy

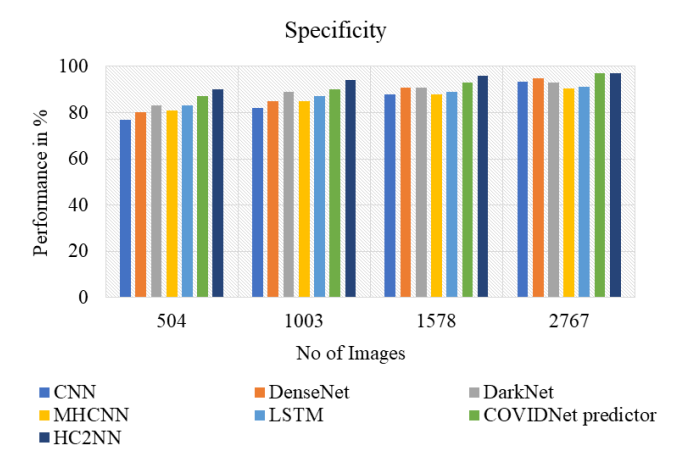


Figure 10: Analysis of Specificity

in terms of mistake rate than alternative algorithms. The proposed HC2NN yields 96% fewer inaccurate results than the current system for CNN of 92.14%, a DenseNet of 93.84%, a DarkNet of 92.21%, a MHCNN of a 91.14%, LSTM of 90.18%, and a COVIDNet predictor of 95.88%.

Figures 12 and 13 represents the validation loss and accuracy plot of the proposed COVIDNet-Predicitor and HC2NN. Validation accuracy typically increases as the model learns from the data, indicating improved performance over time.

The definition of Figures 14 is that when it came to binary classification of either normal chest X-ray images or COVID-19, the HC2NN model—which is trained using full X-ray images—performed the best. It has an F1 score of 0.9505, precision of 0.95, sensitivity of 0.96, specificity of 0.94, and accuracy of 0.9412. The best implementation models' training and testing ROC curves, confusion matrices, training and validation accuracy of 0.9605, and training and validation loss of 91.6.

Discussion

Experimental results show that a deep learning-based COVID-19 identification algorithm has been effectively built using chest X-ray images. The model's good precision, accuracy, recall, and F-measure evaluations showed that it could differentiate between positive and negative COVID-19 cases. Diversifying the training data using several publicly available datasets produces a more potent and broadly applicable model.

Concerns regarding the possible long-term consequences of ionizing radiation, particularly on youngsters, are the main reason for using X-ray scans rather than CT scans. Due to their accessibility and affordability, X-ray scans are a potential option for thorough COVID-19 screening and diagnosis.

Relevant features were effectively retrieved from X-ray images using a CNN design that incorporated convolutional layers, pooling layers, and the ReLU activation function—transfer learning, which significantly enhanced model performance by using pre-trained weights from relevant datasets.

Our COVID-19 detection model showed competitive results when compared to other state-of-the-art techniques, indicating its potential as a valuable weapon in the pandemic response. The model can help speed up the diagnosing process, aid in early detection, and help manage patients by giving radiologists a second view.

Furthermore, it is crucial to recognize the limited quantity and scope of the dataset, even if our work has shown promising results in differentiating between positive and negative cases in chest X-ray photographs using the currently available dataset. Creating a reliable binary classification model is our primary objective. It assesses and acknowledges the possible advantages of using external

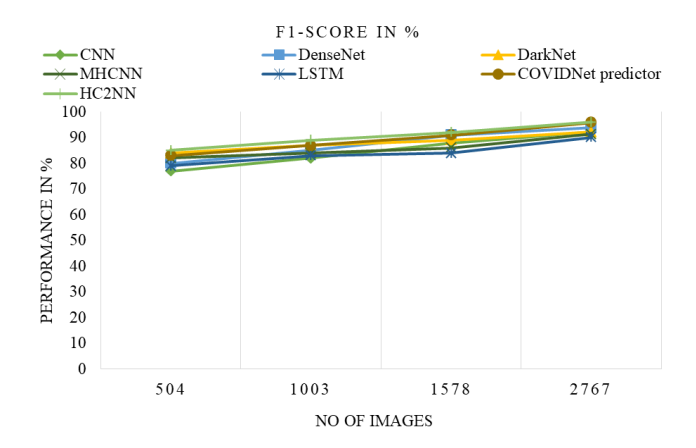


Figure 11: Analysis of F1 score

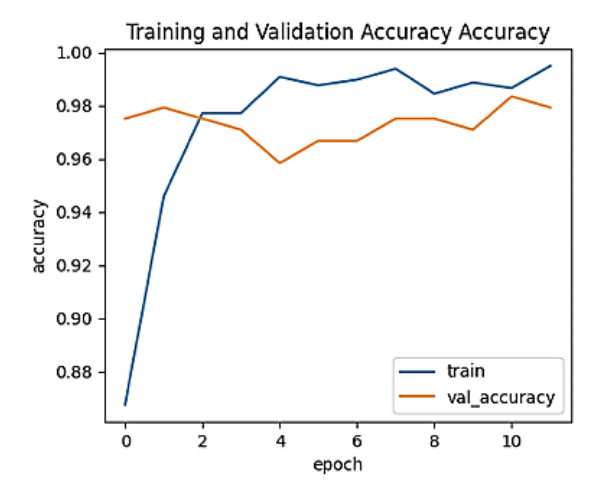


Figure 12: Training and validation accuracy

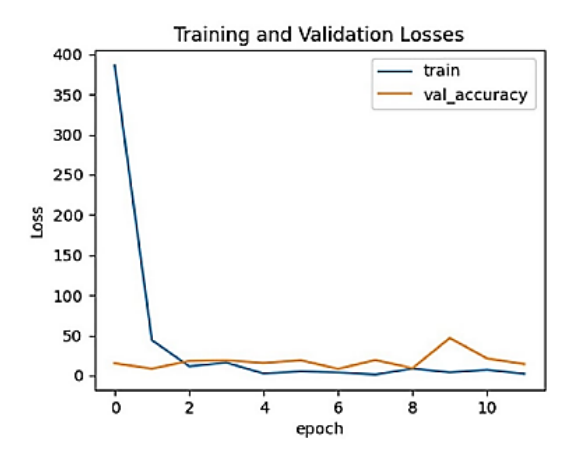


Figure 13: Training and validation loss

datasets to enhance the generalizability of our approach. Itintends to work with medical institutions in subsequent studies to obtain access to more extensive and diverse datasets to expand the scope of our research and solve issues of dataset volume and representativeness.

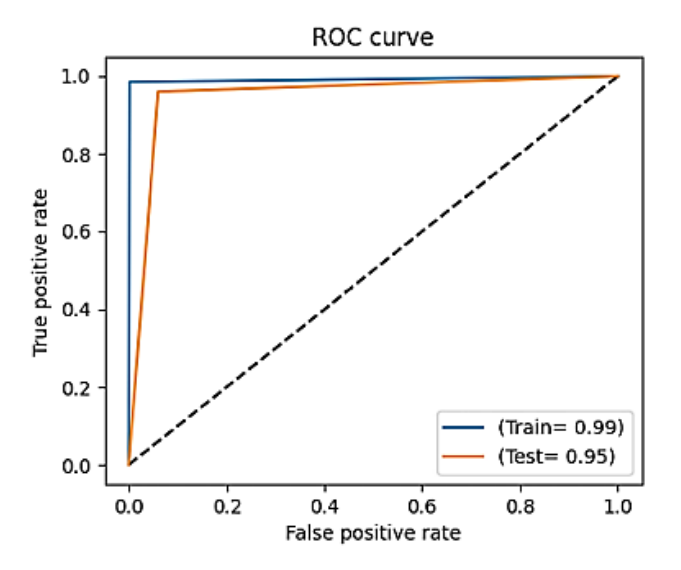


Figure 14: Training ROC curve

Conclusion

Effective treatment of lung cancer, a serious and occasionally fatal illness, depends on early detection. The importance of deep learning, more especially the application of Convolutional Neural Networks, is revolutionizing medical diagnosis. The basic HC2NN model has a lower level of precision because of overfitting in validation and training accuracy. However, deep learning approaches improve diagnosis efficacy and accuracy while reducing the workload of healthcare manual prediction. The model is enhanced via regularization, which raises training and validation accuracy by 5%. However, because the model has a minor overfit, an augmentation strategy is applied to improve accuracy, resulting in a 10% increase in accuracy and reduced overfitting. To detect lung cancer photographs, the authors created a deep learning-based application with an average validation loss of 91.6% and better training and validation accuracy of 0.9605. This technique for detecting lung cancer using CT scans is more adaptable and simple to utilize.

Acknowledgements

I am deeply grateful for the successful completion fo this research article titled "OPTIMIZED DEEP LEARNING FRAMEWORK FOR COVID-19 PREDICTION USING LUNG IMAGING"

I would like to extend my sincere gratitudemy Research Supervisor, Dr. M. Mohamed Surputheen, for his valuable guidance and continuous support throughout this research. I am also grateful to our Co-Research Supervisor, Dr. M. Rajakumar, for his insightful feedback and technical advice. Special thanks to Dr. S. Peerbasha for his expertise and motivation, which greatly enhanced this work and appreciate the contributions of all collaborators and the support from our institution and colleagues, which made this research possible.

References

- Aharonu, M., & Ramasamy, L. (2024). A multi-model deep learning framework and algorithms for survival rate prediction of lung cancer subtypes with region of interest using histopathology imagery. IEEE Access, 12, 155309–155329. https://doi.org/10.1109/ACCESS.2024.3484495
- Babu, N., Pruthviraja, D., & Mathew, J. (2024). Enhancing lung acoustic signals classification with eigenvectors-based and traditional augmentation methods. IEEE Access, 12, 87691–87700. https://doi.org/10.1109/ACCESS.2024.3417183
- Banerjee, N., & Das, S. (2021). Lung cancer prediction in deep learning perspective.
- Bohmrah, M. K., & Kaur, H. (2021). Classification of COVID-19 patients using efficient fine-tuned deep learning DenseNet model. Global Transitions Proceedings, 2(2), 476–483. https://doi.org/10.1016/j.qltp.2021.08.003
- Chetupalli, S. R., Krishnan, P., Sharma, N., Muguli, A., Kumar, R., Nanda, V., Pinto, L. M., Ghosh, P. K., & Ganapathy, S. (2023). Multi-modal point-of-care diagnostics for COVID-19 based on acoustics and symptoms. IEEE Journal of Translational Engineering in Health and Medicine, 11, 199–210.
- Haennah, J. H. J., Christopher, S., & King, R. G. (2023). Prediction of the COVID disease using lung CT images by deep learning algorithm: DETS-optimized ResNet 101 classifier. Precision Medicine, 10. https://doi.org/10.3389/fmed.2023.1157000
- Irtaza, M., Ali, A., Gulzar, M., & Wali, A. (2024). Multi-label classification of lung diseases using deep learning. IEEE Access, 12, 124062–124080. https://doi.org/10.1109/ACCESS.2024.3454537
- Jiang, H., Ma, H., Qian, W., et al. (2017). An automatic detection system of lung nodule based on multigroup patch-based deep learning network. IEEE Journal of Biomedical and Health Informatics, 22, 1227–1237. https://doi.org/10.1109/JBHI.2017.2725903
- Jiang, W., Zeng, G., Wang, S., et al. (2022). Application of deep learning in lung cancer imaging diagnosis. Journal of Healthcare Engineering, 2022, 1–12. https://doi.org/10.1155/2022/6107940
- Kumar, V., & Bakariya, B. (2021). Classification of malignant lung cancer using deep learning. Journal of Medical Engineering & Technology, 45, 85–93. https://doi.org/10.1080/03091902 .2020.1853837
- Liu, S., & Yao, W. (2022). Prediction of lung cancer using gene expression and deep learning with KL divergence gene selection. BMC Bioinformatics, 23. https://doi.org/10.1186/s12859-022-04689-9
- Mathesul, S., Swain, D., Satapathy, S., Rambhad, A., Acharya, B., Gerogiannis, V., & Kanavos, A. (2023). COVID-19 detection from chest X-ray images based on deep learning techniques. Algorithms, 16(10), 494. https://doi.org/10.3390/a16100494
- Ozdemir, O., Russell, R. L., & Berlin, A. A. (2020). A 3D probabilistic deep learning system for detection and diagnosis of lung cancer using low-dose CT scans. IEEE Transactions on Medical Imaging, 39(5), 1419–1429. https://doi.org/10.1109/TMI.2019.2947595
- Ozturk, T., Talo, M., Yildirim, E. A., Baloglu, U. B., Yildirim, O., & Acharya, U. R. (2020). Automated detection of COVID-19 cases using deep neural networks with X-ray images. Computers in Biology and Medicine, 121, Article 103792.
- Peerbasha, S., Mohamed Surputheen, M. (2021). A predictive model

- to identify possible affected bipolar disorder students using Naïve Bayes, Random Forest, and SVM machine learning techniques of data mining and building a sequential deep learning model using Keras. IJCSNS International Journal of Computer Science and Network Security, 21(5), 267–275. https://doi.org/10.22937/IJCSNS.2021.21.5.36
- Pham, L., Phan, H., Palaniappan, R., Mertins, A., & McLoughlin, I. (2021). CNN-MoE based framework for classification of respiratory anomalies and lung disease detection. IEEE Journal of Biomedical and Health Informatics, 25(8), 2938–2947. https://doi.org/10.1109/JBHI.2021.3064237
- Roy, A., & Satija, U. (2023). RDLINet: A novel lightweight inception network for respiratory disease classification using lung sounds. IEEE Transactions on Instrumentation and Measurement, 72, 1–13. https://doi.org/10.1109/TIM.2023.3292953
- Roy, A., Thakur, A., & Satija, U. (2023). VGAResNet: A unified visibility graph adjacency matrix-based residual network for chronic obstructive pulmonary disease detection using lung sounds. IEEE Sensors Letters, 7(11), 1–4. https://doi.org/10.1109/LSENS.2023.3326118
- Sanghvi, H. A., Patel, R. H., Agarwal, A., Gupta, S., Sawhney, V., & Pandya, A. S. (2023). A deep learning approach for classification of COVID and pneumonia using DenseNet-201. International Journal of Imaging Systems and Technology, 33(1), 18–38.
- Tripathy, R. K., Dash, S., Rath, A., Panda, G., & Pachori, R. B. (2022). Automated detection of pulmonary diseases from lung sound signals using fixed-boundary-based empirical wavelet transform. IEEE Sensors Letters, 6(5), 1–4. https://doi.org/10.1109/LSENS.2022.3167121
- Vinta, S. R., Lakshmi, B., Safali, M. A., & Kumar, G. S. C. (2024). Segmentation and classification of interstitial lung diseases based on hybrid deep learning network model. IEEE Access, 12, 50444–50458. https://doi.org/10.1109/ACCESS.2024.3383144
- Wu, C., Ye, N., & Jiang, J. (2024). Classification and recognition of lung sounds based on improved Bi-ResNet model. IEEE Access, 12, 73079–73094. https://doi.org/10.1109/ACCESS.2024.3404657
- Yadav, P., Menon, N., Ravi, V., & Vishvanathan, S. (2023). Lung-GANs: Unsupervised representation learning for lung disease classification using chest CT and X-ray images. IEEE Transactions on Engineering Management, 70(8), 2774–2786. https://doi.org/10.1109/TEM.2021.3103334
- Yu, H., Zhou, Z., & Wang, Q. (2020). Deep learning assisted prediction of lung cancer on computed tomography images using the adaptive hierarchical heuristic mathematical model. IEEE Access, 8, 86400–86410. https://doi.org/10.1109/ACCESS.2020.2992645
- Zaidi, S. Z. Y., Akram, M. U., Jameel, A., & Alghamdi, N. S. (2021). Lung segmentation-based pulmonary disease classification using deep neural networks. IEEE Access, 9, 125202–125214. https://doi.org/10.1109/ACCESS.2021.3110904
- Zhang, X., et al. (2023). CXR-Net: A multitask deep learning network for explainable and accurate diagnosis of COVID-19 pneumonia from chest X-ray images. IEEE Journal of Biomedical and Health Informatics, 27(2), 980–991. https:// doi.org/10.1109/JBHI.2022.3220813